2021 American Control Conference (ACC)
New Orleans, USA, May 25-28, 2021

Attitude Pointing Control using Artificial Potentials with Control Input Constraints

Abhijit Dongare, Reza Hamrah and Amit K. Sanyal[1]

Abstract— **This paper presents a novel approach for pointing direction control of a rigid body with a body-fixed sensor, in the presence of control constraints and pointing direction constraints. This scheme relies on the use of artificial potentials where an attractive artificial potential is placed at the desired pointing direction and a repulsive artificial potential is used to avoid an undesirable pointing direction. The proposed control law ensures almost global asymptotic convergence of the rigid body to its desired pointing direction, while satisfying the control input constraints and avoiding the undesirable pointing direction. These theoretical results are followed by numerical simulation results that provide an illustration of the scheme for a realistic spacecraft pointing control scenario.**

I. Introduction

Active pointing control of a rigid body with a body-fixed exteroceptive imaging sensor, has applications to unmanned aerial, underwater, and space vehicles. In many such applications, there are constraints on the control effort and there may be restrictions (or exclusion zones) for the pointing direction. An example where the latter situation occurs is when an imaging sensor should not be pointed in a direction close to that of the sun. In this paper, we consider pointing control of a rigid body with torque magnitude constraints as well as a pointing direction exclusion zone.

Spacecraft attitude pointing control with sun direction vector avoidance for large angle maneuvers using Euler angles was carried out in [1]. Attitude control for large angle rotations using quaternions are studied, e.g., in [2]. These prior works use feedback of the full attitude state of the rigid body. However, the full attitude state may not always be available or necessary for pointing control. For pointing (boresight) control, the problem is one of *reduced attitude control* of a rigid body, where the configuration space is the sphere $\mathbb{S}^2$, consisting of unit vectors in $\mathbb{R}^3$.

Among the prior literature related to reduced attitude control, [3] is focused on control on $\mathbb{S}^2$ and stabilization of the spacecraft about an unactuated axis of rotation. An extensive study of control on spheres is performed in [4]. In [5], an underactuated spacecraft is asymptotically stabilized using state feedback law. A detailed review of rigid body attitude control, with particular emphasis on stability and stabilization, was provided in [6]. It describes full and reduced attitude control on the configuration spaces $\mathrm{SO}(3)$ and $\mathbb{S}^2$ respectively, and almost global stability on the respective state spaces. Boresight control and guidance is studied in [7], which also discusses different scenarios for applications like pointing, tracking and searching. Other prior research on reduced attitude (or pointing direction) control includes, e.g., [8], [9], [10], and [11].

Constraints in attitude control is another relevant area of research in attitude control with obvious practical applications. Unmanned vehicles and spacecraft can have different types of constraints that limit attitude control inputs, including limits on angular velocity and torque, besides pointing direction constraints. Prior literature has explored different control and state constraints in attitude and reduced attitude control, and solutions to overcome them. Artificial potential functions have been used for navigation of a vehicle towards a desired set or reference, while avoiding obstacles [1], [12], [13]. Undesirable attitude and pointing direction avoidance was studied in [14], using geometric mechanics. A cost function was optimized to ensure the avoidance of an excluded direction. Logarithmic barrier potential functions were used in [15], [16] to avoid exclusion zones in pointing direction. The former work also had a mandatory zone constraint and used a back-stepping controller. The latter work used an adaptive controller to stabilize the system in presence of an unknown disturbance. Another study of exclusion and mandatory zones was given in [17]. Angular velocity constraint along with dynamic pointing constraint was considered in [18]. The velocity constraint was satisfied by limiting the angular velocity error, leading to conservative results. Spacecraft formation control in the presence of attitude and position constraints was considered in [19]. They employed rapidly-exploring random trees for path planning along with a smoother for optimization. The control of an underactuated axisymmetric spacecraft was considered in [20]. A discontinuous control law was designed for asymptotic tracking and stabilization. Note that discontinuous control has practical impediments for spacecraft control, where it may excite structural vibrations in flexible space structures.

Another method to satisfy the control constraints in a control system revolves around the use of reference governors. An approach involving Model Predictive Control was also proposed in [21] to satisfy the control constraints. Both thrust and exclusion zone constraints were considered. A fast solver method for the optimization problem was also proposed. The work in [22], considers actuator saturation and exclusion zones. This is a two step scheme, where a reference trajectory is generated in quaternion space in the first step. Then a reference governor is applied to the pre-stabilized system to satisfy the control constraints. Along the same lines, [23] studies torque and inclusion zone constraints on $\mathrm{SO}(3)$ using an explicit reference governor. However,

[1] Department of Mechanical and Aerospace Engineering, Syracuse University, Syracuse, NY 13244, USA. audongar, rhamrah, aksanyal@syr.edu

2021 American Control Conference (ACC) | 978-1-6654-4197-1/21/$31.00 ©2021 IEEE | DOI: 10.23919/ACC50511.2021.9483350

these schemes often rely on online optimization, for which significant computational power is required to implement in real time. Additionally, these schemes also employ artificial potential-like functions for navigation.

Our approach to pointing control in the presence of control torque and pointing direction constraints, uses smooth artificial potentials and knowledge of maximum permissible angular velocities (or energy level) of the rigid body. The paper is organized as follows. Section II describes the attitude pointing control problem and introduces required notation. Section III describes the artificial potential functions. The attractive potential function is centered at the desired pointing direction. This attracts the body-fixed sensor pointing direction to the desired pointing direction. The repulsive potential function is designed to avoid an undesirable pointing direction. Section IV introduces the control law to achieve the desired goal and the Lyapunov analysis that ensures the almost global asymptotic stability of the desired pointing direction. In Section V, control parameters are designed such that the control input constraints are satisfied for the given system, and the corresponding control law. Section VI presents numerical simulation results to demonstrate the effectiveness of this scheme. Section VII provides concluding remarks with planned future research on this topic.

II. Problem Definition

A. Coordinate Frame Definition

The configuration space of rigid body attitude motion is $\mathrm{SO}(3)$. The attitude is described by a rotation matrix relating a body-fixed coordinate frame to an inertial coordinate frame. We consider a coordinate frame $\mathcal{B}$ fixed to the body and another coordinate frame $\mathcal{I}$ that is fixed in space and takes the role of an inertial coordinate frame. Let $R(t) \in \mathrm{SO}(3)$ denote the time-varying rotation matrix for the rigid body rotating from body fixed frame $\mathcal{B}$ to inertial frame $\mathcal{I}$, where $\mathrm{SO}(3)$ denotes the group of all rotations in $\mathbb{R}^3$.

B. Rigid Body Reduced Attitude Description

Consider a rigid body (e.g. a space telescope) and its attitude dynamics. Let $p \in \mathbb{S}^2$ denote the desired pointing direction for the body fixed sensor in inertial frame. Then $\Gamma = R^{\mathrm{T}}p$ is the desired sensor pointing direction (reduced attitude) resolved in body frame. Without loss of generality, consider $e_1 = [1\ 0\ 0]^{\mathrm{T}} \in \mathbb{S}^2$ to be the boresight (pointing direction) vector of a sensor that is fixed in the body frame $\mathcal{B}$. Therefore, the pointing control objective is to rotate the body such that e_1 coincides with Γ.

Now denote by $v \in \mathbb{S}^2$ an undesirable pointing direction for the rigid body, expressed in inertial frame $\mathcal{I}$. The corresponding undesirable pointing direction resolved in the body frame is given by $\eta = R^{\mathrm{T}}v$. Therefore, the pointing exclusion zone objective is to ensure that e_1 avoids a prescribed exclusion zone around η. This exclusion zone is specified in terms of the angle between e_1 and η, which should be greater than a prescribed angle.

C. Attitude kinematics and Dynamics

Let $\Omega \in \mathbb{R}^3$ be the angular velocity of the rigid body expressed in body frame. The kinematics for the full attitude of the rigid body is given by

$$\dot{R} = R\Omega^{\times}, \tag{1}$$

where $(\cdot)^{\times} : \mathbb{R} \to \mathfrak{so}(3)$ is the skew-symmetric cross product operator and $\mathfrak{so}(3)$ is the Lie algebra of $\mathrm{SO}(3)$, identified with the linear space of 3×3 skew-symmetric matrices. Note that the cross-product operator is given by:

$$x^{\times} = \begin{bmatrix} x_1 \\ x_2 \\ x_3 \end{bmatrix}^{\times} = \begin{bmatrix} 0 & -x_3 & x_2 \\ x_3 & 0 & -x_1 \\ -x_2 & x_1 & 0 \end{bmatrix}. \tag{2}$$

The reduced attitude kinematics equation for the desired pointing direction can be obtained by taking a time derivative of $\Gamma = R^{\mathrm{T}}p$, and substituting the full attitude kinematics (1). Using eq. (1), the reduced attitude kinematics equation is given by:

$$\dot{\Gamma} = \dot{R}^{\mathrm{T}}p = (R\Omega^{\times})^{\mathrm{T}}p = -\Omega^{\times}\Gamma = \Gamma^{\times}\Omega. \tag{3}$$

Similarly, the kinematics equation for the undesirable pointing direction can be obtained by taking a time derivative of both sides of the expression $\eta = R^{\mathrm{T}}v$, as follows:

$$\dot{\eta} = \dot{R}^{\mathrm{T}}v = (R\Omega^{\times})^{\mathrm{T}}v = -\Omega^{\times}\eta = \eta^{\times}\Omega. \tag{4}$$

The attitude dynamics of the system is modeled by

$$J\dot{\Omega} = -\Omega \times J\Omega + \tau_c, \tag{5}$$

where $J \in \mathbb{R}^{3\times 3}$ represents the positive definite inertia matrix of the rigid body defined in frame $\mathcal{B}$, and τ_c is the applied control input torque.

III. Artificial Potential

The main purpose of the artificial potential functions is to help the rigid body achieve its desired pointing direction while avoiding the undesirable pointing directions. This is enabled using the attractive and repulsive artificial potentials on $\mathbb{S}^2$ designed here.

A. Attractive artificial potential function

The body fixed sensor pointing vector on the rigid body is stabilized to the desired pointing direction using an attractive artificial potential. Consider the following attractive artificial potential for the desired pointing direction centered at Γ in frame $\mathcal{B}$:

$$U_a(\Gamma) = k_a(1 - e_1^{\mathrm{T}}\Gamma), \tag{6}$$

where $k_a > 0$ is the control gain value for the attractive function. From the above defining equation (6), we get the maximum and minimum value of the attractive potential function as:

$$\begin{cases} \max\{U_a(\Gamma)_{\Gamma\in\mathbb{S}^2}\} = 2k_a & (\text{when } \Gamma = -e_1), \\ \min\{U_a(\Gamma)_{\Gamma\in\mathbb{S}^2}\} = 0 & (\text{when } \Gamma = e_1). \end{cases} \tag{7}$$

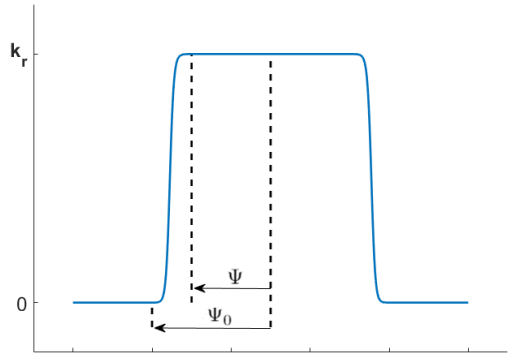

Fig. 1: Representation of Repulsive potential Function

Thus, this function is designed to be a positive definite function on $\mathbb{S}^2$ that has a maximum value when the sensor is pointing opposite to the desired pointing direction and a minimum value when it is pointing along the desired pointing direction. The time derivative of the above equation (6) is given by,

$$\dot{U}_a(\Gamma, \Omega) = -k_a e_1^{\mathrm{T}} \Gamma^{\times} \Omega. \tag{8}$$

B. Repulsive artificial potential function

Undesirable pointing directions can occur in rigid body pointing control applications, e.g., a star tracker sensor on a spacecraft should not be pointed directly towards the sun. To avoid these undesirable directions, repulsive artificial potentials are designed. Consider the following smooth analytical bump function centered at η:

$$U_r(\eta) = \begin{cases} 0 & e_1^{\mathrm{T}}\eta \in [-1, \cos\Psi_0] \\ k_r e^{\frac{-b\beta(\eta)^2}{\gamma^2(\gamma^2-\beta(\eta)^2)}} & e_1^{\mathrm{T}}\eta \in [\cos\Psi_0, \cos\Psi] \\ k_r & e_1^{\mathrm{T}}\eta \in [\cos\Psi, 1] \end{cases} \tag{9}$$

where

$$\begin{aligned} \beta(\eta) &= e_1^{\mathrm{T}}\eta - \cos\Psi \\ \gamma &= \cos\Psi - \cos\Psi_0, \end{aligned} \tag{10}$$

$k_r > 0$ is a control gain value for the repulsive function and b determines the steepness of this function. The angle Ψ is the minimum required angular separation between the undesirable pointing direction and the sensor pointing direction. In the above function, angle Ψ traces an inner circular boundary. The region inside this boundary is restricted region for sensor pointing direction. The angle Ψ_0 describes the influence zone of this function. The representation of the repulsive potential function is given in Fig. 1. The function reaches a maximum value of k_r when $e_1^{\mathrm{T}}\eta = \cos\Psi$. As $e_1^{\mathrm{T}}\eta$ approaches the outer circle (i.e., $e_1^{\mathrm{T}}\eta = \cos\Psi_0$), the function decays to zero and remains zero outside the exclusion zone. The particular design of the repulsive potential in eq. (9) ensures that the function is smooth everywhere on $\mathbb{S}^2$.

Therefore the permissible pointing directions for the body-fixed sensor is given by the set:

$$P_d = \{\Gamma \in \mathbb{S}^2 \mid \Gamma^{\mathrm{T}}\eta < \cos\Psi\}. \tag{11}$$

Note that $U_r(\eta)$ as defined by eq. (9) is continuous, and the value of $U_r(\eta) < k_r$ as long as the desired pointing direction is in the permissible set P_d. As a result, the value of this gain can be set to be the value of the initial value of a Lyapunov function that is decreasing along the dynamics of the feedback system.

The derivative of the above function is

$$\dot{U}_r(\eta, \Omega) = k_r \alpha(\eta) \Omega^{\mathrm{T}} e_1^{\times} \eta, \tag{12}$$

where $\alpha(\eta)$ is defined in a piecewise manner as

$$\alpha(\eta) = \begin{cases} 0 & e_1^{\mathrm{T}}\eta \in [-1, \cos\Psi_0] \\ \dfrac{-2b\beta(\eta)}{k_r\left(\gamma^2 - \beta(\eta)^2\right)^2} U_r(\eta) & e_1^{\mathrm{T}}\eta \in [\cos\Psi_0, \cos\Psi] \\ 0 & e_1^{\mathrm{T}}\eta \in [\cos\Psi, 1]. \end{cases} \tag{13}$$

IV. Control Law

In this section, the control law that guarantees the convergence of the sensor pointing direction to the desired pointing direction is obtained. The Lyapunov stability analysis that ensures the *almost global* asymptotic stability of the desired pointing direction is also presented.

Theorem 1: Consider the kinematics for the desired and undesired pointing directions given in (3) and (4) respectively, and the attitude dynamics equation given in (5). Let $L(t)$ be a positive definite diagonal matrix. Define the attitude control law to be

$$\tau_c = -L(t)\Omega + k_a e_1^{\times}\Gamma - k_r \alpha(\eta) e_1^{\times}\eta, \tag{14}$$

where $\alpha(\eta)$ is defined in (13). Further, let the desired pointing direction be outside the influence zone of the repulsive potential given by the angle Ψ_0. Then the proposed control law stabilizes the body-fixed sensor pointing direction to the desired pointing direction in an asymptotic manner, while avoiding the undesired direction.

Proof: Consider the following candidate Morse-Lyapunov function,

$$V(\Gamma, \eta, \Omega) = \frac{1}{2}\Omega^{\mathrm{T}} J \Omega + U_a(\Gamma) + U_r(\eta) \tag{15}$$

The derivative of this Morse-Lyapunov function $\dot{V}(\Gamma, \eta, \Omega)$, substituting the equations (8), (12) and (13), is given by,

$$\dot{V}(\Gamma, \eta, \Omega) = \Omega^{\mathrm{T}} J \dot{\Omega} - k_a e_1^{\mathrm{T}} \Gamma^{\times} \Omega + k_r \alpha(\eta) \Omega^{\mathrm{T}} e_1^{\times} \eta.$$

Now substituting the attitude dynamics (5), this time derivative simplifies to:

$$\begin{aligned} \dot{V}(\Gamma, \eta, \Omega) &= \Omega^{\mathrm{T}} \left[J\Omega \times \Omega + \tau_c - k_a e_1^{\times}\Gamma + k_r \alpha(\eta) e_1^{\times}\eta \right] \\ &= \Omega^{\mathrm{T}} \left[\tau_c - k_a e_1^{\times}\Gamma + k_r \alpha(\eta) e_1^{\times}\eta \right]. \end{aligned} \tag{16}$$

Note that Ω and $J\Omega \times \Omega$ are orthogonal, and therefore the term $\Omega^{\mathrm{T}}[J\Omega \times \Omega]$ vanishes. After substitution of the control law (14) into eq. (16), $\dot{V}(\Gamma, \eta, \Omega)$ simplifies to:

$$\dot{V}(\Gamma, \eta, \Omega) = \dot{V}(\Omega) = -\Omega^{\mathrm{T}} L(t) \Omega. \tag{17}$$

Given that $L(t) = \mathrm{diag}([l_1(t), l_2(t), l_3(t)])$ where $l_i(t) > 0$ for $i = 1, 2, 3$, the above derivative of the Morse-Lyapunov function is strictly non-increasing. Therefore, $\dot{V}$ is negative semi-definite. Using LaSalle's invariance principle on $\mathrm{T}\mathbb{S}^2$, we conclude that the feedback system is asymptotically stabilized at the desired pointing direction if this direction is outside the zone of influence of the repulsive potential centered at the undesirable direction (in which case $\alpha(\eta) = 0$). Therefore, the body-fixed sensor pointing direction is stabilized to the desired pointing direction, and the given result follows. ∎

V. Control Constraints

This section provides a description of control constraints for the system that are achieved by designing certain control parameters. The design of these parameters ensure that the system stabilizes to the desired pointing direction, while satisfying the control constraints and avoiding the undesired direction.

A. Design of k_r

From equation (9), it is clear that the maximum value of the repulsive potential function is given by the control gain constant k_r. This maximum value occurs along the boundary $e_1^{\mathrm{T}}\eta = \cos(\Phi)$. Now, consider a sub-level set of the state space given by,

$$V(\Gamma, \eta, \Omega) = \frac{1}{2}\Omega^{\mathrm{T}} J \Omega + U_a(\Gamma) + U_r(\eta) \leq V^{\max}. \tag{18}$$

The gain value k_r can be designed in a way such that the sub-level set given by equation (18) becomes invariant. Consider for example the following equations

$$k_r = V^{\max} = k_a(1 - e_1^{\mathrm{T}}\Gamma_I), \tag{19}$$

where $e_1^{\mathrm{T}}\Gamma_I$ gives the initial angular separation. The use of the criteria mentioned above points to the idea that the system will never have the required energy to violate the constraint.

Another noticeable fact is that outside of the exclusion zone we have $U_r(\eta) \equiv 0$, which implies that only the $\Omega^{\mathrm{T}} J \Omega$ and $U_a(\Gamma)$ terms govern the Lyapunov function (15).

B. Design of $L(t)$

Referring to equation (14), it can be deduced that the second and third term are orientation dependent and are bounded. Thus, the control constraints are satisfied by designing the control gain values $l_i(t)$ in the first term $-L(t)\Omega$. Rewriting the control torque equation (14) in the component form we get

$$\begin{Bmatrix} \tau_1 \\ \tau_2 \\ \tau_3 \end{Bmatrix} = \begin{Bmatrix} -l_1(t)\Omega_1 \\ -k_a\Gamma_3 + k_r\alpha(\eta)\eta_3 - l_2(t)\Omega_2 \\ k_a\Gamma_2 - k_r\alpha(\eta)\eta_2 - l_3(t)\Omega_3 \end{Bmatrix}. \tag{20}$$

We consider control torque constraints of the form:

$$-\tau_{i,min} \leq \tau_i \leq \tau_{i,max}, \tag{21}$$

where $\tau_{i,min}, \tau_{i,max} > 0$. Now consider the first component $l_1(t)$. From equation (21), the torque constraint for τ_1 can written as

$$-\tau_{1,min} \leq -l_1(t)\Omega_1 \leq \tau_{1,max}. \tag{22}$$

If we consider $\Omega_1 > 0$, then we have $l_1(t)\Omega_1(t) \leq \tau_{1,min}$ which leads to $l_1(t) \leq \frac{\tau_{1,min}}{\Omega_1(t)}$. And if $\Omega_1 > 0$ then $l_1(t)|\Omega_1(t)| \leq \tau_{1,max}$ which leads to $l_1(t) \leq \frac{\tau_{1,max}}{|\Omega_1(t)|}$. Therefore, the term $l_1(t)$ can be designed as follows

$$l_1(t) = \frac{\tau_{1,m}}{|\Omega_1(t)| + \epsilon_1}, \tag{23}$$

where $\tau_{1,m} = \min\{\tau_{1,min}, \tau_{1,max}\}$ and $\epsilon_1 > 0$ is a small positive number that can be considered a control gain parameter.

Now consider the $l_2(t)$. From (21), second component of torque τ_2 can be written as

$$\begin{aligned} k_a\Gamma_3 - k_r\alpha(\eta)\eta_3 + l_2(t)\Omega_2 &\leq \tau_{2,min} \\ -k_a\Gamma_3 + k_r\alpha(\eta)\eta_3 - l_2(t)\Omega_2 &\leq \tau_{2,max}. \end{aligned}$$

If we consider $\Omega_2 > 0$ then we have

$$l_2(t) \leq \frac{\tau_{2,min} - k_a\Gamma_3 + k_r\alpha(\eta)\eta_3}{\Omega_2(t)}.$$

Likewise for $\Omega_2 < 0$

$$l_2(t) \leq \frac{\tau_{2,max} + k_a\Gamma_3 - k_r\alpha(\eta)\eta_3}{|\Omega_2(t)|}.$$

A conservative design of $l_2(t)$ therefore is of the form

$$l_2(t) = \frac{\tau_{2,m} - |k_a\Gamma_3 - k_r\alpha(\eta)\eta_3|}{|\Omega_2(t)| + \epsilon_2}, \tag{24}$$

where $\tau_{2,m} = \min\{\tau_{2,min}, \tau_{2,max}\}$ and $\epsilon_2 > 0$ is a small positive control gain parameter.

Similarly $l_3(t)$ is also designed. From (21), third component of torque τ_3 is of the form

$$\begin{aligned} -k_a\Gamma_2 + k_r\alpha(\eta)\eta_2 + l_3(t)\Omega_3 &\leq \tau_{3,min} \\ k_a\Gamma_2 - k_r\alpha(\eta)\eta_2 - l_3(t)\Omega_3 &\leq \tau_{3,max}. \end{aligned}$$

The design of $l_3(t)$ is given by

$$l_3(t) = \frac{\tau_{3,m} - |k_a\Gamma_2 - k_r\alpha(\eta)\eta_2|}{|\Omega_3(t)| + \epsilon_3}, \tag{25}$$

where $\tau_{3,m} = \min\{\tau_{3,min}, \tau_{3,max}\}$ and $\epsilon_3 > 0$ is a small positive control gain parameter.

Thus equations (23), (24) and (25) give positive but time-varying gains with the assumption that $\tau_{i,m} > 0$. Since $l_1(t)$, $l_2(t)$, and $l_3(t)$ are positive, one can conclude from equations (24) and (25) it is evident that

$$\begin{aligned} &\tau_{2,m} - |k_a\Gamma_3 - k_r\alpha(\eta)\eta_3| > 0 \text{ and} \\ &\tau_{3,m} - |k_a\Gamma_2 - k_r\alpha(\eta)\eta_2| > 0. \end{aligned} \tag{26}$$

This leads to a condition where the control parameters for attractive and repulsive potential function in equation (6) and (9) respectively should satisfy the relation

$$\tau_{i,m} > k_a + \alpha(\eta) k_r.$$

Using (13) the above equation can be written as

$$\tau_{i,m} - k_a > \frac{-2b\beta(\eta)}{\left(\gamma^2 - \beta(\eta)^2\right)^2} U_r(\eta). \tag{27}$$

A value of b can be obtained that satisfies the above relation.

The following section presents numerical results obtained by implementing the scheme proposed in this paper for attitude pointing control and guidance of a rigid body with a body-fixed sensor.

VI. Simulation Results

This section presents numerical simulation results for the scheme proposed in this paper for attitude pointing control using artificial potential fields. These simulation results are provided for a time period of $T = 40s$, and with time step size of $\Delta t = 0.01s$, to demonstrate the performance of the proposed pointing control scheme.

The initial conditions and other parameters used for this simulation are described here. The sensor pointing direction in the body-fixed frame is $e_1 = [1 \ 0 \ 0]^{\mathrm{T}}$. The initial attitude and angular velocity of the rigid body is given by $R = I$, and $\Omega_0 = [0 \ 0 \ 0]^{\mathrm{T}}$ in the body frame, respectively. The desired pointing direction in the inertial frame is $p = [-0.866 \ 0 \ 0.5]^{\mathrm{T}}$. The initial and final pointing directions are 150° apart. The undesirable pointing direction in the inertial frame is $v = [0 \ 0.28 \ 0.96]^{\mathrm{T}}$. The minimum required angular separation between the sensor pointing direction and undesired pointing direction is $\Psi = 20^\circ$ and the influence zone for the repulsive potential begins at $\Psi_0 = 30^\circ$. The control torque limits are set to $\tau_{\max} = [2 \ \ 2 \ \ 2]^{\mathrm{T}}$ Nm and $-\tau_{\min} = [-2 \ \ -2 \ \ -2]^{\mathrm{T}}$ Nm. Based on eq. (27), the value of $b = 0.18$ is selected as appropriate. Also, the control gains for the angular velocity feedback are set to $\epsilon_1 = \epsilon_2 = \epsilon_3 = 0.5$.

The results of the simulation are summarized in Fig. 2 and Fig. 3. The plot in Fig. 2a shows the reduced attitude error as the angular separation between current sensor pointing direction and desired pointing direction. From the parameters considered for this simulation, the initial angular separation between the sensor pointing direction and the desired pointing direction is 150°, as reflected in the plot. This error converges to zero asymptotically, as the sensor pointing direction converges to the desired direction. Plots of torque components in Fig. 2b show that the torque values are confined to the given upper and lower limits. Therefore, we see that this design of control gain parameters maintains the torque constraints. Except for the transients in torque values at approximately $t = 4.5$ s, the absolute values are well below the limits. The plots in Fig. 2c show the convergence of the angular velocities of the rigid body. Based on the theoretical development, the control gains l_1, l_2, and l_3 are designed so that they are positive, as shown in Fig. 2d. The transients in the results at approximately $t = 4.5$ s occur when the sensor enters the influence zone of the repulsive potential and then changes direction to move away from it.

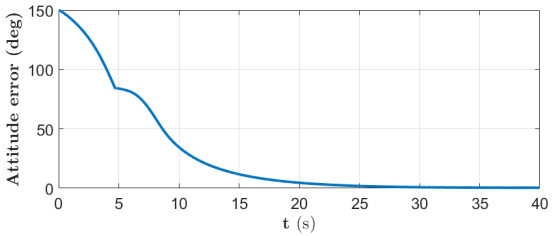

(a) Attitude error in degrees

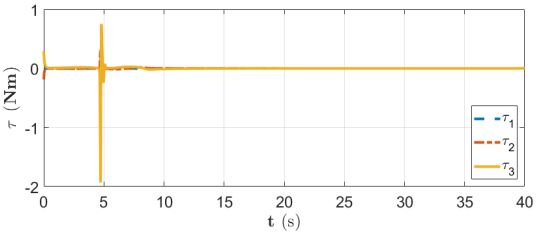

(b) Torque

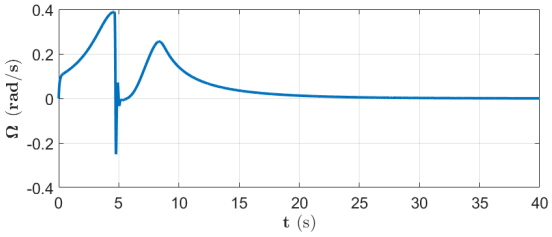

(c) Angular Velocity

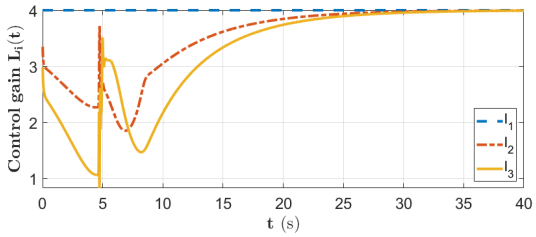

(d) Control Gain Values

Fig. 2: Simulation Results for $\Delta t = 0.01$ and $t_f = 40s$.

Fig. 3 shows the time evolution of the sensor pointing direction on $\mathbb{S}^2$, as it orients itself to achieve the desired pointing direction. There is a shaded region inside the inner circular boundary which specifies the restricted zone for sensor pointing direction. The outer circular boundary indicates the beginning of the repulsive potential influence zone. The sensor pointing direction enters the repulsive potential influence zone but eventually moves away from it. The design of the control gain parameters will dictate how deep the sensor pointing direction will penetrate inside this influence zone, while the control constraints remain satisfied. The sensor then exits the influence zone to converge to the

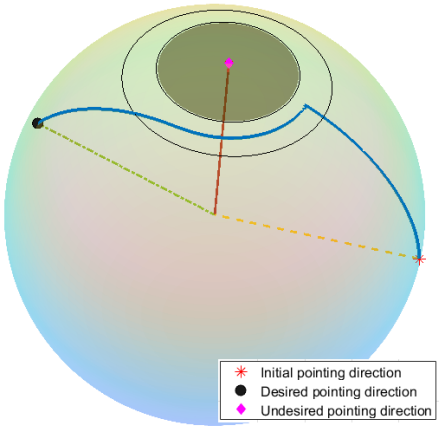

Fig. 3: Trajectory traced by the sensor pointing direction as evolution of time

desired pointing direction.

VII. Conclusion

This paper presents a novel scheme for attitude pointing control and guidance of a rigid body with a body fixed sensor. The sensor has to avoid an exclusion zone around an undesirable pointing direction, and is subject to control torque constraints. This scheme relies on the use of an attractive artificial potential to guide the sensor to its desired pointing direction and a repulsive potential to avoid the undesirable pointing direction. A Lyapunov stability analysis for the proposed control law guarantees almost global asymptotic stability of the sensor pointing direction at the desired pointing direction. The control parameters are designed so that they satisfy the control input and pointing direction exclusion zone constraints. Numerical simulations demonstrate the validity of this scheme. The results also show maintenance of the input torque constraints, as a result of the design of control gain parameters. Future research will consider pointing direction (reduced attitude) tracking of the body fixed sensor and techniques to make the control torque inputs less conservative.

Acknowledgement

The authors acknowledge support from the National Science Foundation awards CISE 1739748. and IIP 1938518 (SBIR through Akrobotix, LLC).

References

[1] C. R. Mclnnes, "Large angle slew maneuvers with autonomous sun vector avoidance," *Journal of Guidance, Control, and Dynamics*, vol. 17, no. 4, pp. 875–877, 1994. [Online]. Available: https://doi.org/10.2514/3.21283

[2] B. Wie and P. M. Barba, "Quaternion feedback for spacecraft large angle maneuvers," *Journal of Guidance, Control, and Dynamics*, vol. 8, no. 3, pp. 360–365, 1985. [Online]. Available: https://doi.org/10.2514/3.19988

[3] F. Bullo, R. Murray, and A. Sarti, "Control on the sphere and reduced attitude stabilization," *IFAC Proceedings Volumes*, vol. 28, no. 14, pp. 495 – 501, 1995, 3rd IFAC Symposium on Nonlinear Control Systems Design 1995, Tahoe City, CA, USA, 25-28 June 1995. [Online]. Available: http://www.sciencedirect.com/science/article/pii/S1474667017468789

[4] R. W. Brockett, "Lie theory and control systems defined on spheres," *SIAM Journal on Applied Mathematics*, vol. 25, no. 2, pp. 213–225, 1973. [Online]. Available: https://doi.org/10.1137/0125025

[5] C. I. Byrnes and A. Isidori, "On the attitude stabilization of rigid spacecraft," *Automatica*, vol. 27, no. 1, pp. 87 – 95, 1991. [Online]. Available: http://www.sciencedirect.com/science/article/pii/000510989190008P

[6] N. A. Chaturvedi, A. K. Sanyal, and N. H. McClamroch, "Rigid-body attitude control," *IEEE Control Systems Magazine*, vol. 31, no. 3, pp. 30–51, June 2011.

[7] C. M. Pong and D. W. Miller, "Reduced-attitude boresight guidance and control on spacecraft for pointing, tracking, and searching," *Journal of Guidance, Control, and Dynamics*, vol. 38, no. 6, pp. 1027–1035, 2015. [Online]. Available: https://doi.org/10.2514/1.G000264

[8] P. Tsiotras and J. M. Longuski, "Spin-axis stabilization of symmetric spacecraft with two control torques," *Systems & Control Letters*, vol. 23, no. 6, pp. 395 – 402, 1994. [Online]. Available: http://www.sciencedirect.com/science/article/pii/0167691194900930

[9] N. A. Chaturvedi, N. H. McClamroch, and D. S. Bernstein, "Asymptotic smooth stabilization of the inverted 3-d pendulum," *IEEE Transactions on Automatic Control*, vol. 54, no. 6, pp. 1204–1215, June 2009.

[10] H. Krishnan, M. Reyhanoglu, and H. McClamroch, "Attitude stabilization of a rigid spacecraft using two control torques: A nonlinear control approach based on the spacecraft attitude dynamics," *Automatica*, vol. 30, no. 6, pp. 1023 – 1027, 1994. [Online]. Available: http://www.sciencedirect.com/science/article/pii/0005109894901961

[11] N. A. Chaturvedi and N. H. McClamroch, "Asymptotic stabilization of the hanging equilibrium manifold of the 3d pendulum," *International Journal of Robust and Nonlinear Control*, vol. 17, no. 16, pp. 1435–1454, 2007. [Online]. Available: https://onlinelibrary.wiley.com/doi/abs/10.1002/rnc.1178

[12] U. Lee and M. Mesbahi, "Feedback control for spacecraft reorientation under attitude constraints via convex potentials," *IEEE Transactions on Aerospace and Electronic Systems*, vol. 50, no. 4, pp. 2578–2592, 2014.

[13] S. Kulumani and T. Lee, "Constrained geometric attitude control on so(3)," *International Journal of Control, Automation and Systems*, vol. 15, no. 6, pp. 2796–2809, 2017.

[14] K. Spindler, "Attitude maneuvers which avoid a forbidden direction," *Journal of Dynamical and Control Systems*, vol. 8, no. 1, pp. 1–22, 2002.

[15] U. Lee and M. Mesbahi, "Spacecraft reorientation in presence of attitude constraints via logarithmic barrier potentials," in *Proceedings of the 2011 American Control Conference*, 2011, pp. 450–455.

[16] S. Kulumani and T. Lee, "Constrained geometric attitude control on SO(3)," *International Journal of Control, Automation and Systems*, vol. 15, no. 6, 2017.

[17] H. B. Hablani, "Attitude commands avoiding bright objects and maintaining communication with ground station," *Journal of Guidance, Control, and Dynamics*, vol. 22, no. 6, pp. 759–767, 1999. [Online]. Available: https://doi.org/10.2514/2.4469

[18] Q. Hu, B. Chi, and M. R. Akella, "Reduced attitude control for boresight alignment with dynamic pointing constraints," *IEEE/ASME Transactions on Mechatronics*, vol. 24, no. 6, pp. 2942–2952, 2019.

[19] I. Garcia and J. P. How, "Trajectory optimization for satellite reconfiguration maneuvers with position and attitude constraints," in *Proceedings of the 2005, American Control Conference, 2005.*, 2005, pp. 889–894 vol. 2.

[20] P. Tsiotras and J. Luo, "Control of underactuated spacecraft with bounded inputs," *Automatica*, vol. 36, no. 8, pp. 1153 – 1169, 2000. [Online]. Available: http://www.sciencedirect.com/science/article/pii/S000510980000025X

[21] R. Gupta, U. V. Kalabić, S. Di Cairano, A. M. Bloch, and I. V. Kolmanovsky, "Constrained spacecraft attitude control on SO(3) using fast nonlinear model predictive control," in *2015 American Control Conference (ACC)*, 2015, pp. 2980–2986.

[22] M. M. Nicotra, D. Liao-McPherson, L. Burlion, and I. V. Kolmanovsky, "Spacecraft attitude control with nonconvex constraints: An explicit reference governor approach," *IEEE Transactions on Automatic Control*, vol. 65, no. 8, pp. 3677–3684, 2020.

[23] S. Nakano, T. W. Nguyen, E. Garone, T. Ibuki, and M. Sampei, "Attitude constrained control on SO(3): An explicit reference governor approach," in *2018 IEEE Conference on Decision and Control (CDC)*, 2018, pp. 1833–1838.